Electronic Supplementary Material (ESI) for Metallomics.

A Set of Robust Fluorescent Peptide Probes for Quantification of Cu(II) Binding Affinities in the Micromolar to Femtomolar Range

Tessa R. Young, Chathuri J. K. Wijekoon, Benjamin Spyrou, Paul S. Donnelly, Anthony G. Wedd and Zhiguang Xiao*

School of Chemistry and Bio21 Molecular Science and Biotechnology Institute, University of Melbourne, Parkville, Victoria 3010, Australia

E-mail: z.xiao@unimelb.edu.au

Tel.: (61 3) 9035 6072; Fax: (61 3) 9347 5180

Electronic Supplementary Information

Characterisation of Probes DP1-4

Probe DP1

The data from titration of low micromolar concentrations of DP1 indicated the existence of a Cu(II) binding equilibrium at Cu : DP1 ~ 1 : 1 (Fig. 4b; eqn 1). The titration curves for $[DP1]_{tot}$ = 2.0 μM at two different MOPS buffer concentrations of 5.0 and 0.5 mM were indistinguishable, indicating that the buffer made an insignificant contribution to the Cu(II) binding at such ratio of DP1 to MOPS. An apparent $\log K_D^{'} = -8.0 \pm 0.1$ for Cu^{II}-DP1 under these conditions was derived from global curve-fittings to eqn 4 of the two sets of titration data at $[DP1]_{tot}$ = 2.0 and 0.20 μM (Table 2). F_1 was defined by the optimised curve-fitting as detailed in the experimental section (Fig. 4b; Table 1).

It was also possible to determine a conditional K_D for Cu^{II}-DP1 via ligand competition using Gly as a competing affinity standard (Table S1; Fig. S1). The determination is based on eqns 6a, 7a and 8 with the pre-condition of negligible contributions from both Cu_{aq}^{2+} and 'Cu^{II}-B' to the total Cu(II) speciation. To enforce this requirement and avoid dilution effects, series of solutions were prepared in a minimum concentration of MOPS buffer (5.0 mM, pH 7.4). They contained a fixed concentration of $Cu^{II}_{0.8}$-DP1 but increasing concentrations of competing ligand Gly. The fluorescence intensity increased with increasing Gly, and reached a final value characteristic of the original *apo*-DP1 form (Fig. 4c). Consequently, the terms $[Cu^{II}P]$ and $[Cu_{aq}^{2+}]$ could be estimated reliably via eqn 5 and eqn 7a, allowing curve fitting to eqn 8 and extraction of the estimate $\log K_D = -8.1 \pm 0.2$ for Cu^{II}-DP1 at pH 7.4 (Fig. 4d). This value is in good agreement with the apparent $\log K_D^{'} = -8.0 \pm 0.1$ derived above via direct metal ion titration and consolidates the reliability of both approaches. It confirms that the buffer MOPS at low concentrations exerted an insignificant effect on the Cu(II) speciation analysis of the direct metal ion titration. A conditional $\log K_D = -8.1$ was adopted which is

connected to the log K_D = −10.1 for DP2 favorably via effective competition of either probe for Cu(II) with the Ac-Aβ16 peptide (Fig. 10a,b; Table 3).

Probe DP2

The affinity of the first site is too high (K_D too small) to be determined via direct metal ion titration due to the detection limit of the probe concentration (~ 0.1 μM). Consequently, the affinity was determined via ligand competition with both Gly and His as affinity standards (Fig. 5b,c), as described for DP1. Both analyses provided log K_D = −10.1 ± 0.1 at pH 7.4, an affinity higher by about 2 orders of magnitude than that of DP1 (Table 2). The increased affinity allowed application of the higher affinity Cu(II) ligand His as an independent standard at about 100-fold lower concentration (Fig. 5b; Table S1). This led an essentially identical logK_D (Fig. 5d; Table 2), highlighting the reliability of the approach and the robustness of the probe. Equivalent competition experiments were carried out with both 2.0 μM and 10.0 μM probe solution to give the same K_D value, demonstrating that the derived dissociation constant is independent of probe concentration.

Equivalent experiments were conducted at lower and higher pH in buffers of MES (50 mM, pH 6.2) and CHES (50 mM, pH 9.2) and consistent K_D values were obtained based on either affinity standard of Gly or His in both buffers (logK_D = −8.0 at pH 6.2 and −12.5 at pH 9.2; Table 2). In comparison to the logK_D = −10.1 at pH 7.4, the Cu(II) affinity at pH 6.2 decreased by 2.1 orders of magnitude while that at pH 9.2 increased by 2.4 orders of magnitude. The affinity decrease by ~ 100 times from pH 7.4 to 6.2 is consistent with a Cu(II) site involving pH-sensitive ligands N-terminal nitrogen (pK_a = 8.0−8.5) and two His side-chains (pK_a ~ 6.5) as Cu(II) ligands, but an affinity increase by 2.4 orders of magnitude from pH 7.4 to 9.2 is not consistent with the same set of binding ligands, suggesting that at least one peptide backbone nitrogen must be recruited for Cu(II) binding at high pH. A supporting

evidence is provided by the characteristic F_1/F_0 value that is different at low and high pH solution (Table 1). Indeed, various spectroscopic evidences support a Cu(II) binding site transition in similar Aβ16 peptide at pH ~7.8.[1] As expected, the extensively studied Aβ16 and its derivative Aβ16wwa possess comparable Cu(II) affinities and similar pH effect (*vide infra*).

Probe DP4

DP4 was designed to bind Cu(II) with a binding site similar to that of DP3 (Fig. 3a) but with higher affinity. However, unexpectedly, DP4 was proved to adopt the classic ATCUN binding mode within the pH range 6.2-9.2 shown in Fig. 3b. This claim is based on following experimental evidences with control experiments conducted using DP3 that is proved to bind Cu(II) in a non-ATCUN mode (see text and Fig. 3b) and DAHK peptide that was demonstrated vigorously to bind Cu(II) in the ATCUN binding mode.[2]

(i) Both Cu(II)-DP4 and Cu(II)-DAHK, but not Cu(II)-DP3, exhibit characteristic *d-d* transitions with an absorption maximum at $\lambda \sim 525$ nm (Fig. 2), a fingerprint for the presence of an ATCUN Cu(II) centre in the complexes.[3] This spectral feature is persistent even in more acidic solution of pH 6.2, demonstrating unchanged binding mode at low pH.

(ii) The EPR spectrum of Cu(II)-DP4 is very similar to that of Cu(II)-DAHK, but these are somewhat different from that of Cu(II)-DP3 (Fig. S7, Table S3). EPR spectrum is sensitive to the equatorial ligands mainly for Cu(II) complexes. Similar to the cases of DP3 and DAHK, the EPR spectrum of Cu(II)-DP4 remains essentially unchanged within the pH range 6.2-9.2 (Fig. S7), consistent with the observation of an unchanged fluorescence quenching index of F_1/F_0 (= 0.09) for DP4 within this pH range (Table 1).

(iii) The visible CD spectra of Cu(II)-DP4 and Cu(II)-DAHK at pH 7.4 are intense and very similar, but the spectrum of Cu(II)-DP3 is weak and very different (Fig. S8). However, unfortunately, it was not possible to identify the His to Cu(II) and amide to Cu(II) charge transfer bands in the near UV region for DP probes due to the intense absorbance of the dansyl group at $\lambda < 400$ nm (Fig. 2).

(iv) In contrast to the case of DP3, binding of Cu(II) to DP4 increases its affinity to the anion-exchange column (Fig. 6), suggesting a net increase in negative charge due to Cu(II) binding and supporting an ATCUN binding mode that demands deprotonation of the N-terminal ammonium and the two intervening peptide amide nitrogen ligands (Fig. 3b).

(v) The $\log K_D$ of Cu(II)-DP4 is much more sensitive to pH than that of Cu(II)-DP3, but is comparable to that of Cu(II)-DAHK (Fig. 7). In fact, the relationship between $\log K_D$ and pH cannot be fitted to eqn S2 within the pH rang 6.2-9.2, indicating that the Cu(II) site involves at least one ligand with $pK_a > 9.2$.

This combined evidence confirms that Cu(II)-DP4 features an ATCUN Cu(II) centre shown in Fig. 3b. Apparently, addition of the potential side-chain ligands of His1 and His4 in DP4 relative to the sequence of DAHK is not able to offer a sufficient thermodynamical advantage for a non-ATCUN binding mode and the high energy cost for deprotonation of the two intervening peptide amide ligands must be compensated fully by the formation of three favourable chelate rings of 6, 5 and 6 members (Fig. 3b). Indeed, the affinity of DP4 for Cu(II) is only marginally higher than that of DAHK (Tables 2, 3), suggesting relatively small contributions (if any) of the side-chains of His1 and His4 to the Cu(II) binding. They may function as axial ligand(s).

Probe Aβ16wwa

This probe was developed recently for quantification of the Cu(II) binding affinities of other Aβ peptides.[4] The Cu(II) affinity of Aβ16wwa itself was calibrated with Gly as an affinity standard, as is also the case for current probes DP1 and DP2, but the detection relied on the fluorescent emission of Trp with excitation at ~280 nm, instead of the less interfering fluorescence of the dansyl group. In this work, the Cu(II) K_D of Aβ16wwa at pH 7.4 was re-calibrated with new probe DP2 and was found to have a good agreement with the previous value ($\log K_D = -9.9$ vs -9.8; Fig. S6c,d; Table 2). The Cu(II) affinities of Aβ16wwa at low and high pH were determined similarly with DP2 probe and they are $\log K_D = -7.7 \pm 0.2$ and -12.5 ± 0.1 at pH 6.2 and 9.2, respectively. These values differ from the value $\log K_D = -9.9$ at pH 7.4 by 2.2 and 2.6, respectively, highly comparable to the similar pH dependency of $\log K_D$ for DP2 (Table 2) and reflecting their similar Cu(II) binding sites.

Previously we attempted but were not able to determine, via direct metal ion titration, the apparent $K_D^{'}$ value for Aβ16wwa at pH 7.4 since the expected $K_D^{'}$ value is much lower than the detection concentration limit of the probe.[4] Current work with DP2 probe determined $K_D = 10^{-7.7}$ M at pH 6.2 that becomes accessible to the direct metal ion titration approach and provides another opportunity for an independent validation of our ligand competition approach with DP probes. Experiments and data processes were conducted equivalently to those for determination of the apparent $K_D^{'}$ of DP1 at pH 7.4 via direct metal ion titration (c.f., Fig. 3a,b vs S6a,b). The determined value of $\log K_D^{'} = -7.9 \pm 0.2$ is in a good agreement to the conditional $\log K_D$ determined via ligand competition with DP2. This agreement echoes a similar match between the two approaches for DP1 at pH 7.4 (Table 2), confirms little buffer effect of MES and MOPS buffers at 5 mM and validates the data acquired in Table 2.

Table S1. Formation constants of several Cu(II) ligands quoted in this work [a]

L	Equilibria	pK_A^H for H^+	log($^{abs}K_A$) for Cu(II)	log(K_A) for Cu(II) at pH		
				6.2	7.4	9.2
Gly	HL/H·L	9.57				
	H_2L/H·HL	2.33				
	$Cu^{II}L/Cu^{II}$·L		8.19	4.82	6.02	7.67
	$Cu^{II}L_2/Cu^{II}L$·L		6.91	3.54	4.74	6.39
His	HL/H·L	9.10				
	H_2L/H·HL	6.05				
	$Cu^{II}L/Cu^{II}$·L		10.16	7.03	8.43	9.91
	$Cu^{II}L_2/Cu^{II}L$·L		7.91	4.78	6.18	7.66
Egta	HL/H·L	9.40				
	H_2L/H·HL	8.79				
	$Cu^{II}L/Cu^{II}$·L		17.7	11.9	14.3	17.2
Hedta	HL/H·L	9.87				
	H_2L/H·HL	5.38				
	$Cu^{II}L/Cu^{II}$·L		17.4	13.7	14.9	16.7

[a] Quoted from ref [5]. The conditional formation constant K_A at a given pH was calculated via following equation:

$$K_A = {}^{abs}K_A\,(1 + K_{A1}^H[H] + K_{A1}^H K_{A2}^H[H]^2 + \cdots)^{-1} \qquad \text{Eqn. S1}$$

where $^{abs}K_A$ is the absolute formation constant and K_{A1}^H and K_{A2}^H are the first and second protonation constant, respectively.

An alternative format of eqn S1 is eqn S2 that describes the relationship between conditional dissociation constant K_D, absolute dissociation constant $^{abs}K_D$ and proton ionization constant pK_a of the coordination ligand(s):

$$K_D = {}^{abs}K_D\,(1 + 10^{pK_{a1}-pH} + 10^{pK_{a1}+pK_{a2}-2pH} + \cdots) \text{ Eqn. S2}$$

Table S2. Conditional dissociation constants (logK_D) of Cu^{II}-DP complexes at varying pH [a]

Probe	logK_D at pH [a]							Affinity standard
	6.2	6.6	6.9	7.4	8.0	8.5	9.2	
DP1	–	–	–	−8.1	−9.4	−10.4	−11.6	Gly
DP2	−8.0	−8.6	−9.2	−10.0	−10.9	−11.6	−12.4	His
DP3	−10.1	−10.8	−11.3	−12.3	−12.9	−13.3	−13.4	Gly/His
DP4	−11.1	−12.1	−12.8	−14.1	−15.5	−16.6	−18.0	His/Egta

[a] The logK_D data were determined via ligand competition for Cu(II) between each probe and the specified affinity standard in respective buffer (50 mM) of MES (pH 6.2, 6.6, 6.9), MOPS (pH 7.4, 8.0), HEPES (pH 8.5) and CHES (pH 9.2). Where more than one affinity standards were used to yield comparable but not identical logK_D values, an average logK_D value was assumed.

Table S3. EPR parameters derived from spectra [a]

Complex	$g_{\parallel}$ [b]	$g_{\perp}$ [b]	$A_{\parallel}$ (G) [b]
Cu^{II}-DP3	2.242	2.060	182
Cu^{II}-DP4	2.178	2.050	200
Cu^{II}-DAHK	2.183	2.049	200
	2.19 [c]	2.04 [c]	199 [c]

[a] see Fig. S7 for sample conditions and instrument recording conditions;
[b] EPR parameters $g_{\parallel}$, $g_{\perp}$ and $A_{\parallel}$ for the Cu(II) complex of each peptide (DP3, DP4, DAHK) recoded at the different pH values (of 6.2, 7.4 and 9.2) were indistinguishable (see Fig. S7); [c] quoted from ref 2.

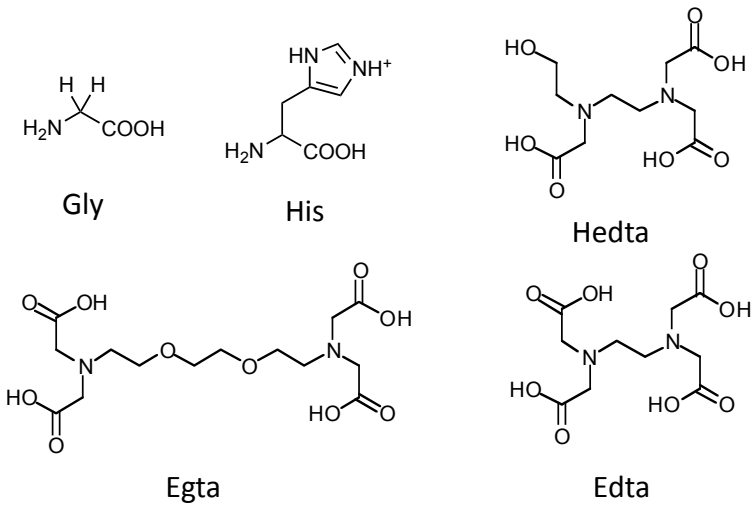

Fig. S1 Structures of Cu(II) ligands used in this work.

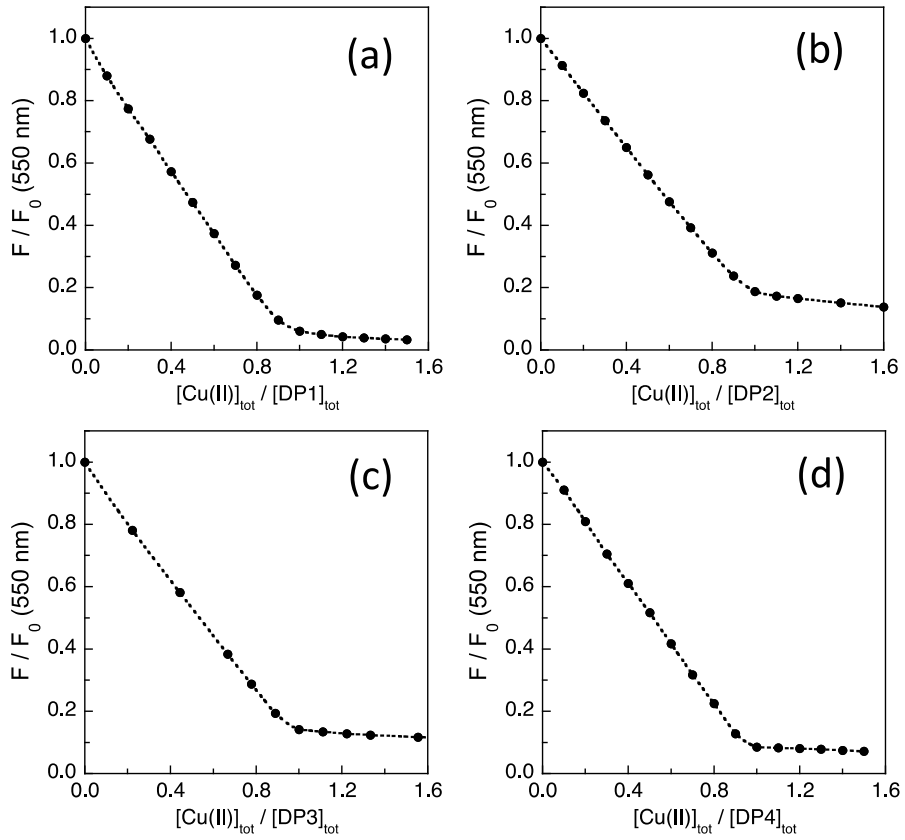

Fig. S2 Calibration of probe concentrations via fluorescence titration of each DP probe with a $CuSO_4$ standard: (a) titration of DP1 (20 μM) in CHES buffer (5.0 mM, pH 9.2); (b) titration of DP2 (10 μM) in MOPS buffer (50 mM, pH 7.4); (c) titration of DP3 (2.0 μM) in MOPS buffer (50 mM, pH 7.4), (d) titration of DP4 (2.0 μM) in MOPS buffer (50 mM, pH 7.4).

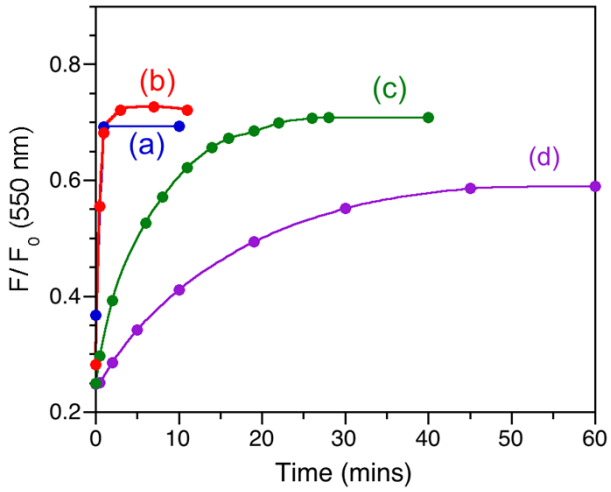

Fig. S3 Cu(II)-exchange rates in MOPS buffer (50 mM, pH 7.4): (a) Cu^{II}-DP2 and Hedta; (b) Cu^{II}-DP3 and Hedta; (c) Cu^{II}-DP4 and His; (d) Cu^{II}-DP4 and Hedta.

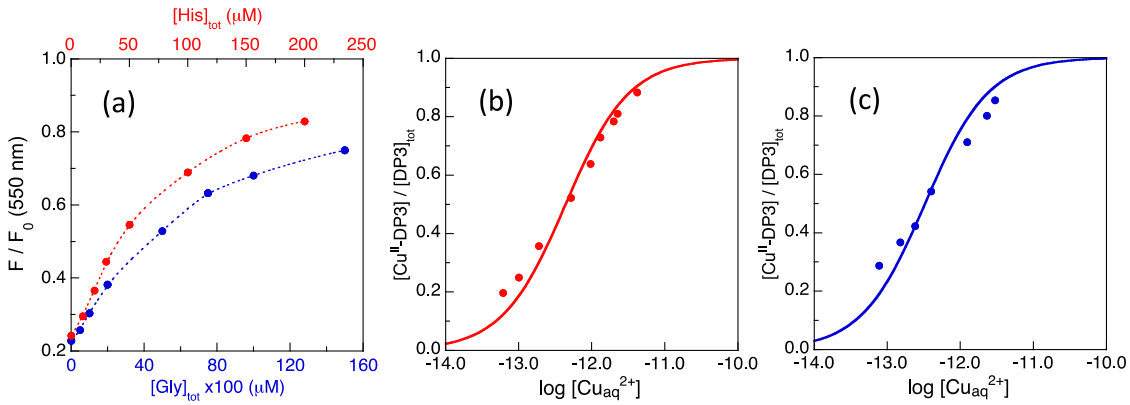

Fig. S4 Determination of the conditional K_D for Cu^{II}-DP3 by competition with ligand Gly or His in MOPS buffer (50 mM, pH 7.4): (a) recovery of F(550) of $Cu^{II}_{0.8}$-DP3 (2.0 μM) with increasing concentration of competing ligand Gly (in blue on bottom scale) or His (in red on top scale); (b, c) curve fittings of $[Cu^{II}\text{-DP3}]/[DP3]_{tot}$ versus $\log[Cu_{aq}^{2+}]$ to eqn 8 derived an consistent estimate of $\log K_D = -12.3 \pm 0.1$ for Cu^{II}-DP3 with either competing ligand His (b) or Gly (c).

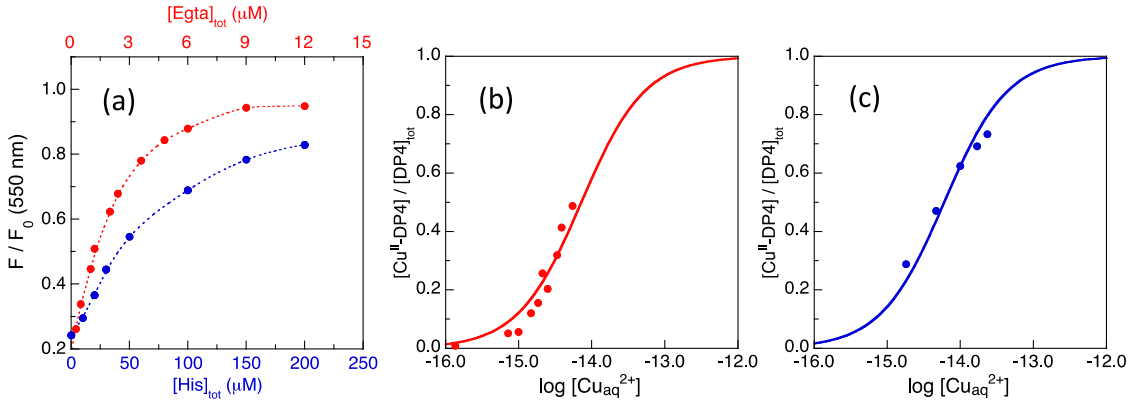

Fig. S5 Determination of the conditional K_D for Cu^{II}-DP4 by competition with ligand His or Egta in MOPS buffer (50 mM, pH 7.4): (a) recovery of F(550) of $Cu^{II}_{0.8}$-DP4 (2.0 μM) with increasing concentration of competing ligand His (in blue on bottom scale) or Egta (in red on top scale); (b, c) curve fittings of $[Cu^{II}\text{-DP4}]/[DP4]_{tot}$ versus $\log[Cu_{aq}^{2+}]$ to eqn 8 derived an consistent estimate of $\log K_D = -14.1 \pm 0.1$ for Cu^{II}-DP4 with either competing ligand Egta (b) or His (c).

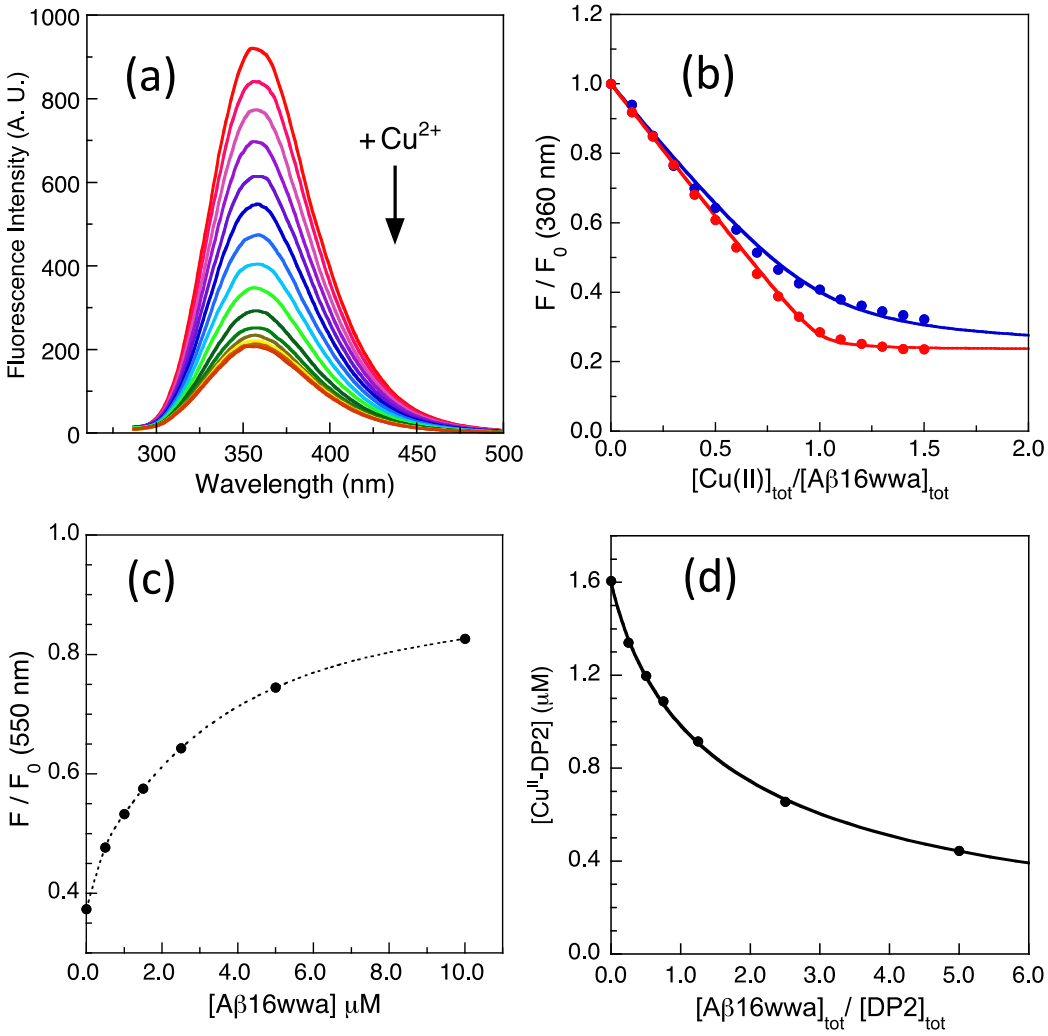

Fig. S6 Determination of apparent $K_D^{'}$ for Cu^{II}-Aβ16wwa by direct metal ion titration (a,b) and of conditional K_D by ligand competition (c,d) in MES buffer (5.0 mM, pH 6.2): (a) quenching of fluorescence emission intensity of Aβ16wwa (2.0 μM) upon titration with Cu^{2+} solution (50 μM); (b) change in F(360) of Aβ16wwa (0.2 μM in blue; 2.0 μM in red) as a function of $[Cu(II)]_{tot}/[Aβ16wwa]_{tot}$. The solid traces are the fitting curves of the experimental data to eqn (4) that allowed derivation of a consistent $\log K_D^{'} = -7.9 \pm 0.2$; (c) recovery of F(550) for $Cu^{II}_{0.8}$-DP2 (2.0 μM) with increasing concentration of competing ligand Aβ16wwa; (d) curve fitting of correlation between $[Cu^{II}\text{-DP2}]$ and $[Aβ16wwa]_{tot} / [DP2]_{tot}$ to eqn 8 derived an estimate of conditional $\log K_D = -7.7 \pm 0.1$ for Cu^{II}-Aβ16wwa.

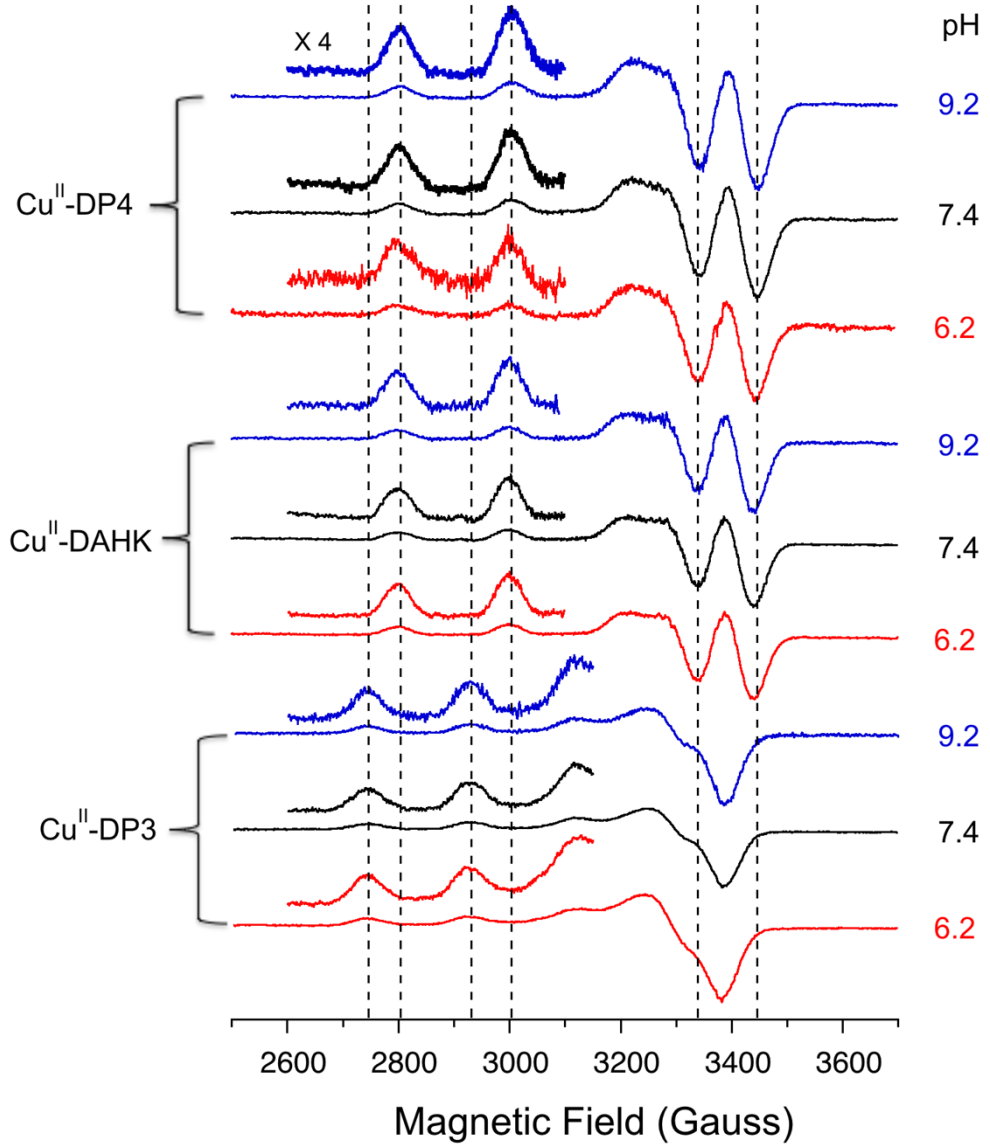

Fig. S7 Frozen solution EPR spectra recorded at 77 K for the Cu(II) complexes of DP3, DP4 and DAHK peptides (0.5 mM; 0.2 mL) at pH 6.2 (red traces), pH 7.4 (black traces) and pH 9.2 (blue traces). Insets show enlargements of the spectra scaled up by a factor of 4. All solutions prepared in 50 mM buffer (Mes pH 6.2; Mops pH 7.4 or Ches pH 9.2) with 10 % glycerol. EPR recording conditions: microwave frequency 9.475 GHz, microwave power 0.633 mW, modulation amplitude 4 G, sweep time 40 s, time constant 20 ms, average number of scans 10.

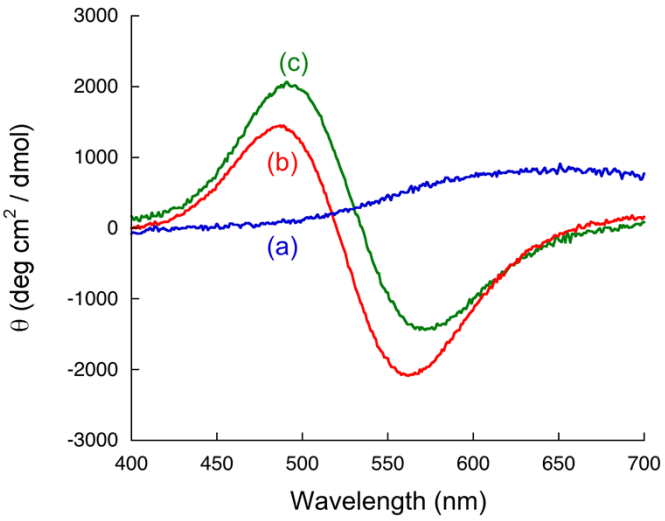

Fig. S8 Visible CD spectra of Cu(II) complexes of DP3 (a); DP4 (b) and DAHK (c) (each 0.3 mM) in Mops buffer (50 mM, pH 7.4) recorded in cell with a pathlength = 1.0 cm.

References

1 C. Hureau, Coordination of redox active metal ions to the amyloid precursor protein and to amyloid-β peptides involved in Alzheimer disease. Part 1: An overview, *Coord. Chem. Rev.,* 2012, **256**, 2164-74.

2 C. Hureau, H. Eury, R. Guillot, C. Bijani, S. Sayen, P.-L. Solari, E. Guillon, P. Faller and P. Dorlet, X-ray and Solution Structures of Cu^{II}-GHK and Cu^{II}-DAHK Complexes: Influence on Their Redox Properties, *Chem.-Eur. J.,* 2011, **17**, 10151-60.

3 C. Harford and B. Sarkar, Amino Terminal Cu(II)- and Ni(II)-Binding Motif of Proteins and Peptides: Metal Binding, DNA Cleavage, and Other Properties, *Acc. Chem. Res.,* 1997, **30**, 123-30.

4 T. R. Young, A. Kirchner, A. G. Wedd and Z. Xiao, An Integrated Study of the Affinities of the Aβ16 Peptide for Cu(I) and Cu(II): Implications for the Catalytic Production of Reactive Oxygen Species, *Metallomics,* 2014, **6**, 505-17.

5 A. E. Martell and R. M. Smith, *NIST Critically Selected Stability Constants of Metal Complexes Database 46, Version 8.0*; U.S. Dept. of Commerce, NIST Standard Reference Data Program: Gaithersburg, MD, 2004.